

Experimental performance investigation of compound parabolic cavity receiver having single absorber tube

Omar Al-Nabhani^a, Saud Al-Kalbani^b, Azzam Al-Alawi^c and Afzal Husain^{*}

Department of Mechanical and Industrial Engineering, Sultan Qaboos University, Muscat, Oman

(Received July 15, 2021, Revised September 4, 2022, Accepted September 7, 2022)

Abstract. The current study presents experimental research on a parabolic trough collector with tube and cavity receivers. The primary concentrating parabolic reflector is designed for an aperture area of 2×2 m² with mirror-polished stainless steel sheet reflectors. The cavity receiver consists of a compound parabolic secondary reflector and a copper tube. Both the conventional tube receiver and the cavity receiver tube are coated with black powder. The experiments are carried out to compare the efficiency of the cavity receiver with the tube receiver for fluid temperature rise, thermal efficiency, and overall losses. The experiments showed significantly higher fluid temperature rise and overall efficiency and lower thermal losses for the cavity receiver compared to the tube receiver within the parameters explored in this study.

Keywords: cavity receiver; compound parabola; parabolic trough concentrator; temperature rise; thermal efficiency; thermal losses

1. Introduction

Solar energy represents a ceaseless source of renewable energy that can be utilized for domestic to industrial applications. However, it is not straightforward due to its low intensity. The intensity of radiation is enhanced with the help of concentrated collectors, i.e., parabolic trough collector (PTC) and Linear Fresnel Collector (LFC). In these devices, radiation is collected and then reflected and received on a receptor called the receiver. However, heat loss in the conversion process is the most common problem for these receivers, which are subjected to a variety of losses and temperature non-uniformity due to uneven solar flux received at their surface (He *et al.* 2019). A cavity receiver (CR) encompasses the wider area where the rays coming from the primary PTC fall on it and reflect on the receiver tube confined within it. The efficiency of the CR depends on its shape and material. It is always required to come up with innovative designs to enhance the efficiency of the receiver.

Different CR shapes and sizes have been proposed and researched over the past decades; however, there is no consensus on the best shape of a CR. Zhu *et al.* (2014) reviewed different

*Corresponding author, Associate Professor, E-mail: afzal19@squ.edu.om

^aStudent, E-mail: s120289@student.squ.edu.om

^bStudent, E-mail: s120289@student.squ.edu.om

^cStudent, E-mail: s120987@student.squ.edu.om

shapes of secondary reflectors or CRs and discussed their advantages and shortcomings. Various shapes have been investigated in the past to optimize the optical efficiency (η_{opt}); however, it was observed that the η_{opt} depends on several other factors of the system related to size and arrangements.

Tsekouras *et al.* (2018) numerically found the optical and thermal characteristics of a CR of trapezoidal shape with a single tube and selective coating for a linear Fresnel collector. It was revealed that the losses increase with the increase in fluid inlet temperature and absorber tube diameter. Hack *et al.* (2017) proposed an adaptive design CR and compared its performance with the most commonly used designs, i.e., compound parabolic concentrator, trapezoidal, and butterfly CR. The trapezoidal CR stands out the best for fabrication easiness; however, the proposed adaptive design showed better thermal performance compared to other receivers investigated by the authors.

Further, Dabiri *et al.* (2018) numerical investigated the outcomes of a trapezoidal cavity angle and the size of the tube. The heat transfer to the tube walls remains unaffected by the increase in tube size, and the heat flow through the cavity increases with the increase in cavity angle. Ortega (2010) invented a CR design consisting of a longitudinally extending tube with a selective coating and fins for enhanced heat transfer. The concave shape receiver chamber is used with a transparent cover in the proposed design. The receiver chamber helps in retaining the incident radiation while the transparent cover protects against convection heat losses. Lin *et al.* (2014) carried out experiments for four CRs, i.e., triangular, arc-shaped, rectangular, and semi-circular. The authors applied a black chrome coating to reduce convection and radiation losses. Moreover, the phenolic foam was used to pack the absorbers and set them within a SS frame consisting of two copper pipes to carry away absorbed heat. The triangular-shaped CR exhibited the best optical and overall performance, and the thermal losses were minimum for an arc-shaped CR.

Lakshmipathy *et al.* (2020) conducted experiments with improved solar cavity collectors. The authors designed five CRs and placed them at equal distances in a metallic box. It was observed that using copper is better than light-weight metal aluminum for receivers. The rectangular cavities exhibited the best performance in preventing heat losses due to stored heat at the corners. Kumar and Reddy (2008) numerically investigated three designs of CRs and compared their thermal performance. The authors found that the redesigned CR outperformed the convectional CR and semi-cavity receiver while changing the facing angle of the receiver from 0° to 90° . Mohamad and Ferrer (2021) proposed a CR with hot mirror coating at the aperture to reduce radiation losses and higher retention of infrared in the cavity space. The efficiency and infrared retention increase with the increase in hot mirror reflectivity. Further, it is observed that the efficiency is increased with the reduction of aperture size at higher temperatures. However, CRs without hot mirror coating and selective coating on the receiver tube has performed better at lower temperatures.

Li *et al.* (2019) numerically studied the effectiveness of a newly proposed linear CR for PTC constructed from a crescent-shaped channel of an alloy with high thermal conductivity. The shape is similar to an evacuated collector tube; however, it has the advantage of developing higher temperature and low maintenance than the evacuated tube collector over long-term use. Cao *et al.* (2016) used a numerical method to model temperature-induced stress and deformation of the tube receiver due to the non-uniform distribution of heat flux on the tube receiver. The stresses are developed due to the difference in temperatures of the inner and outer surfaces of the tube. The maximum deformation of 3.1 mm was observed at 0.82 m in length. Badar *et al.* (2015) numerically investigated tubular CRs having smooth and corrugated inner surfaces with single- and double-glazed aperture windows, and compared the optical performance. The application of

the proposed absorber tube increased the thermal efficiency, and it increased further with the mass flow rate of the heat transfer fluid. The double-glazed aperture exhibited higher efficiency at a higher temperature while at a lower temperature single-glazed surface exhibited higher efficiency.

In the present study, a CR having compound parabolic secondary reflectors and an absorber tube (bare receiver tube) with chrome coating is investigated for its overall thermal performance under realistic solar conditions in Oman. The concentrated parabolic trough is used as a primary reflector.

2. Geometric details and experimental methodology

Fig. 1(a) shows a schematic of a compound parabolic CR with a primary parabolic trough reflector. It consists of two parabolic secondary reflectors, a receiver tube, and a casing with insulation. The diameter and length of the absorber tube are 38.1 mm and 2 m, respectively, and it is made of copper. The absorber tube is painted with a black powder coating to increase the absorptivity. The primary and secondary reflectors are fabricated with a mirror-polished stainless-steel sheet of 0.5 mm thickness. The secondary reflector is used to reflect the falling radiation and direct them to the tube surface. Tempered glass of 0.88 mm thickness is used to cover the CR aperture area to reduce convection losses. The glass cover keeps the heat inside the CR and increases the heat absorption rate. The holders of the CR and the side frame are made of plywood. The holders are used to support the secondary reflectors and the glass cover. The side frame is used to support the tube. The outer box is made of an aluminum sheet of 1.5 mm thickness. It is also used to protect the insulating material from damage in case of exposure to the sun or rain. Fig. 1(b) shows an assembly of different parts of the CR. Fig. 2 shows the conventional receiver tube and the CR.

The experimental system consists of a primary concentrating PTC, CR, reservoir tank, circulating pump, control valves, Pyranometer, thermocouples, and data logger as shown in Fig. 3.

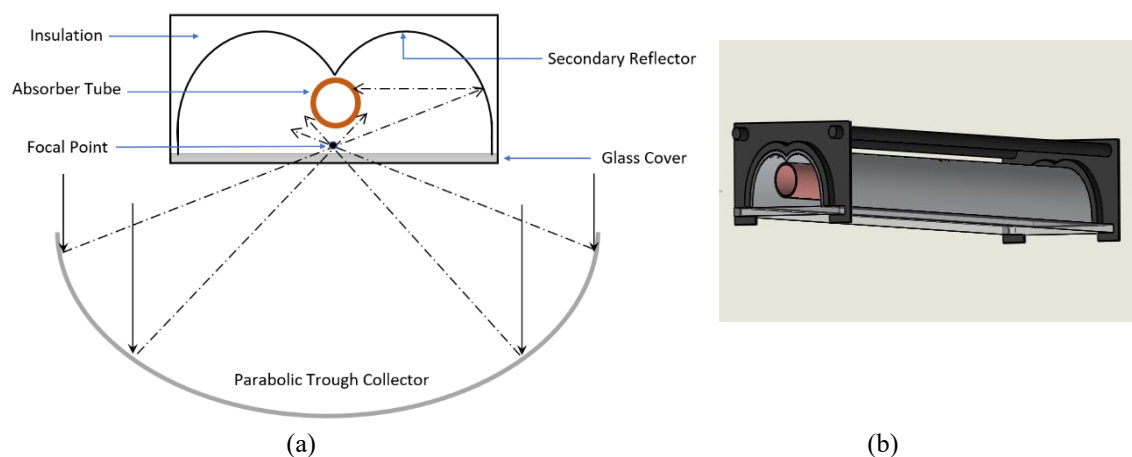


Fig. 1 (a) Schematic of the compound parabolic cavity receiver and (b) 3-D assembly of cavity receiver



(a) (b)
Fig. 2 (a) Conventional tube receiver, (b) cavity receiver

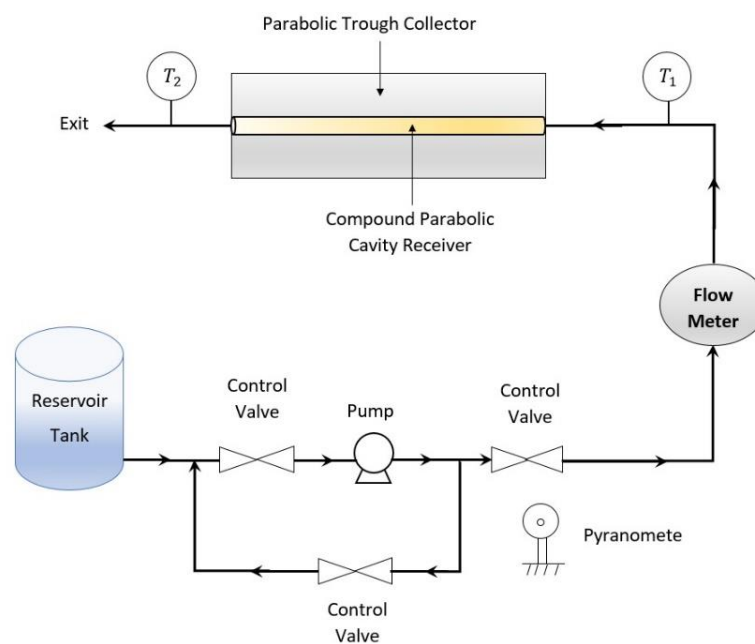


Fig. 3 Schematic of experimental set up for parabolic trough collector system with cavity receiver

The primary PTC is designed for an aperture area of $2 \times 2 \text{ m}^2$ and it is made of a mirror-polished stainless steel sheet. The stand for the entire collector is made of iron and painted black. The Pico Tech data logger with RTD sensors is used to measure the inlet and outlet water temperatures. A validated Hall effect flow sensor with a digital signal transmitter is used to measure the flow rate. An Apogee Pyranometer is used to measure solar insolation.

The experiments are conducted to find out the efficiency of the PTC with a conventional receiver tube and a CR. Water is used as a heat transfer fluid in all experiments. The water flow rate is varied with a control valve. The experimental data is recorded at an interval of 15 minutes after changing the flow rate allowing the temperature to rise and attain a near-steady state. The inlet and outlet fluid temperatures, air temperature, wind velocity, and solar flux are measured at several flow rates.

The thermal efficiency of the tube receiver and cavity receiver is determined by dividing the power obtained by the power of solar heat flux as shown in the following equation

$$\eta = \frac{Q_{gain}}{Q_{solar}} \times 100 \quad (1)$$

Where η is the thermal efficiency, Q_{gain} is the energy absorbed by the working fluid and Q_{solar} is the solar energy fell at the collector. The energy absorbed by the fluid can be represented as

$$Q_{gain} = \dot{m} C_p \Delta T \quad (2)$$

where mass flow rate $\dot{m} = \rho \times \dot{V}$, here \dot{V} is the flow rate. The C_p is the specific heat and ΔT is the temperature rise along the collector tube. The temperature rise can be defined as

$$\Delta T = T_{out} - T_{in} \quad (3)$$

Where T_{out} and T_{in} are the fluid outlet and inlet temperatures, respectively. The solar energy received by the collector can be written as

$$Q_{solar} = q_{solar} \times A \quad (4)$$

where q_{solar} is the incident solar flux. The aperture area (A) of the concentrating PTC is equal to 4 m^2 . The heat loss can be defined as

$$Q_{loss} = Q_{solar} - Q_{gain} \quad (5)$$

The temperature rise per unit of solar flux can be calculated as

$$\theta = \frac{\Delta T}{q_{solar}} \quad (6)$$

3. Results and discussion

The experiments are performed and the data are collected for solar flux, flowrate, inlet, outlet and ambient temperatures, and wind speed. Tables 1 and 2 present the data collected through experiments on two different days for the tube receiver and cavity receiver, respectively. The T_a represents ambient temperature.

The results were deduced for the temperature rise per unit of solar heat flux for both tube receiver and cavity receiver setup by changing flow rate as shown in Fig. 4. The CR shows a higher temperature rise compared to the bare tube receiver throughout the flowrate range explored in this study. The temperature rise decreases monotonously with the increase in flow rates for both cases; however, the rate of decrease is more in cavity receiver arrangement compared to bare tube receiver, and eventually, both bare tube and cavity receivers approach almost the same temperature difference at a high flow rate.

The thermal losses reduce with the increase in flow rate in both bare tube receiver and cavity receiver as shown in Fig. 5. However, the losses are reduced at a faster rate in the tube receiver compared to the cavity receiver. The area exposed to convection losses to the surrounding is higher for the cavity receiver compared to the tube receiver, which leads to higher convection losses under the comparable surface temperature resulting from a higher flow rate. At the higher flow rate,

Table 1 Experimental data of tube receiver for varying flow rate

Time (hours)	Solar Flux (W/m ²)	Flow Rate (L/h)	T _{in} (°C)	T _{out} (°C)	T _a (°C)	Wind Speed (m/s)
10:00 AM	859	30	33	44.66	40.8	1.8
10:15 AM	909.1	51	33.16	42.37	41.26	1.53
10:30 AM	896.6	79.2	33.22	41.31	41.17	1.3
10:45 AM	897.9	109.2	33.28	40.2	40	1.03
11:00 AM	893.6	132	33.32	39.09	39.99	1.52

Table 2 Experimental data of cavity receiver for varying flow rate

Time (hours)	Solar Flux (W/m ²)	Flow Rate (L/h)	T _{in} (°C)	T _{out} (°C)	T _a (°C)	Wind Speed (m/s)
10:30 AM	962.1	34.2	30.2	53.2	39.67	1.83
10:45 AM	963.2	54	30.1	47	38.6	1.62
11:00 AM	961.7	78	30.13	43.2	38.56	1.6
11:15 AM	977.8	100.8	30.34	40.97	38.72	1.62
11:30 AM	984.6	121.2	30.5	38.7	41.16	1.34
11:45 AM	979.2	140.4	30.68	37.6	41.3	1.56

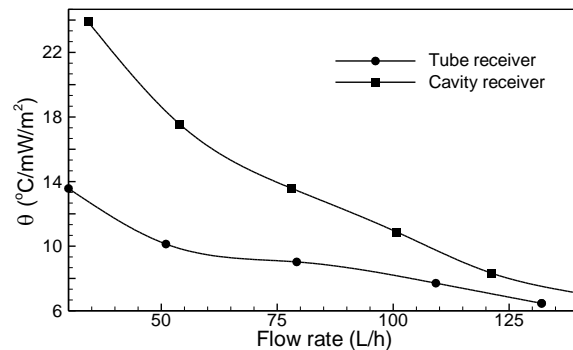


Fig. 4 Fluid temperature rise per unit of solar flux for tube receiver and cavity receiver with the change in flow rates

the capacity of the fluid increases, resulting in a lower fluid temperature and consequently a lower tube surface temperature under the nearly equal heat flux. The lower tube surface temperature resulted in lower convection and radiation losses.

The thermal efficiency of both the bare tube and cavity receivers increases monotonously with the increase in flow rate (Fig. 6). The efficiency of the CR is higher compared to the bare tube receiver throughout the flow rate explored in this study. However, the efficiency of the bare tube receiver approaches the efficiency of the cavity receiver at higher flow rates. Furthermore, as indicated in Figs. 4 and 5, the convection and radiation losses reduce with the increase in flow rate due to the decrease in surface temperature.

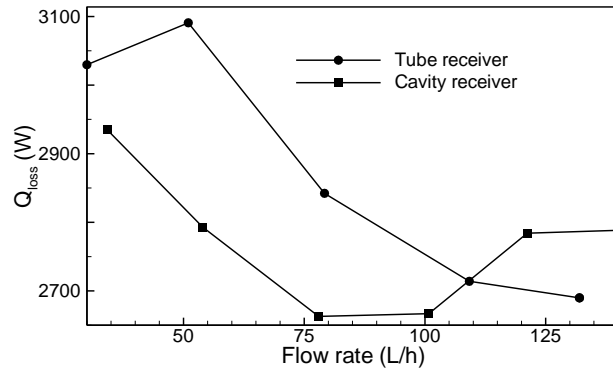


Fig. 5 Thermal losses from the tube and cavity receiver with the change in flow rates

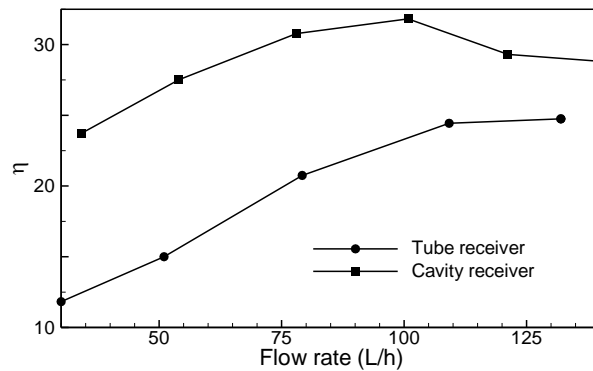


Fig. 6 Efficiency for tube and cavity receivers with the change in flow rates

4. Conclusions

The current study investigates the performance of the CR and compares it with a tube receiver over a range of flow rates and solar flux conditions. A concentrating parabolic trough is used as a primary reflector for both receivers and experiments were conducted to generate the performance data. The cavity receiver is fabricated with the compound parabolic secondary reflectors made of mirror-polished stainless steel sheets with a single receiver tube. The cavity receiver outperforms the tube receiver in several aspects of thermal performance. The cavity receiver generates a significantly higher temperature of working fluid compared to the tube receiver. The cavity receiver reduces overall losses significantly at low flow rates and exhibits significantly high thermal efficiency over the range of flow rates explored in this study. However, the advantages associated with the cavity receiver are more dominant at low flow rates of the working fluid. The maximum temperature rise for the bare tube and cavity receivers were 11.7°C and 23°C at flow rates of 30 L/h and 34.2 L/h, respectively under the incidence solar flux values of 859 W/m² and 962.1 W/m², respectively. The maximum efficiencies for tube and cavity receivers are 24.7% and 31.8%, respectively at flow rates of 132 L/h and 100.8 L/h, respectively, under the solar flux

conditions of 893.6 W/m² and 977 W/m², respectively, as explored in the present study. This indicates the advantage of the cavity receiver in generating higher temperatures for lower flow rate applications.

Acknowledgments

The authors acknowledge the support from Sultan Qaboos University, Oman, (Grant No. (IG/ENG/MEID/21/01) for conducting this research.

References

- Bader, R., Pedretti, A., Barbato, M. and Steinfeld, A. (2015), "An air-based corrugated cavity-receiver for solar parabolic trough concentrators", *Appl. Energ.*, **138**, 337-345. <https://doi.org/10.1016/j.apenergy.2014.10.050>.
- Cao, F., Li, Y., Wang, L. and Zhu, T.Y. (2016), "Thermal performance and stress analyses of the cavity receiver tube in the parabolic trough solar collector". *IOP Conference Series: Earth and Environmental Science*, **40**(1). <https://doi.org/10.1088/1755-1315/40/1/012067>.
- Dabiri, S., Khodabandeh, E., Poorfar, A.K. and Mashayekhi, R. (2018), "Parametric investigation of thermal characteristic in trapezoidal cavity receiver for a linear Fresnel solar collector concentrator", *Energy*, **153**, 17-26. <https://doi.org/S0360544218306297>.
- Hack, M., Zhu, G. and Wendelin, T. (2017), "Evaluation and comparison of an adaptive method technique for improved performance of linear Fresnel secondary designs", *Appl. Energ.*, **208**, 1441-1451. <https://doi.org/10.1016/j.apenergy.2017.09.009>.
- He, Y.L., Wang, K., Qiu, Y., Du, B.C., Liang, Q. and Du, S. (2019), "Review of the solar flux distribution in concentrated solar power: non-uniform features, challenges, and solutions", *Appl. Therm. Eng.*, **149**, 448-474. <https://doi.org/10.1016/j.applthermaleng.2018.12.006>.
- Lakshminpathy, B., Sivaraman, B., Senthilkumar, M., Kajavali, A. and Sivakumar, K. (2020), "Technological improvement on energy-efficient methods applied to a solar cavity collector", *Mater. Sci. Energ. Technol.*, **3**, 456-463. <https://doi.org/10.1016/j.mset.2020.02.010>.
- Li, X., Chang, H., Duan, C., Zheng, Y. and Shu, S. (2019), "Thermal performance analysis of a novel linear cavity receiver for parabolic trough solar collectors", *Appl. Energ.*, **237**, 431-439. <https://doi.org/10.1016/j.apenergy.2019.01.014>.
- Lin, M., Sumathy, K., Dai, Y.J. and Zhao, X.K. (2014), "Science direct performance investigation on a linear fresnel lens solar collector using cavity receiver", *Solar Energ.*, **107**, 50-62. <https://doi.org/10.1016/j.solener.2014.05.026>.
- Mohamad, K. and Ferrer, P. (2021), "Thermal performance and design parameters investigation of a novel cavity receiver unit for parabolic trough concentrator", *Renew. Energ.*, **168**, 692-704. <https://doi.org/10.1016/j.renene.2020.12.089>.
- Ortega (2010), "(12) Patent Application Publication (10) Pub . No .: US 2010 / 0035098 A1 Patent Application Publication" **1**(19), 1-5. <https://patentimages.storage.googleapis.com/3b/c9/82/c283c7b24afe69/US20100019677A1.pdf>.
- Sendhil Kumar, N. and Reddy, K.S. (2008), "Comparison of receivers for solar dish collector system", *Energ. Convers. Manage.*, **49**(4), 812-819. <https://doi.org/10.1016/j.enconman.2007.07.026>.
- Tsekouras, P., Tzivanidis, C. and Antonopoulos, K. (2018), "Optical and thermal investigation of a linear fresnel collector with trapezoidal cavity receiver", *Appl. Therm. Eng.*, **135**, 379-388. <https://doi.org/10.1016/j.applthermaleng.2018.02.082>.
- Zhu, G., Wendelin, T., Wagner, M.J. and Kutscher, C. (2014), "History, current state, and future of linear

fresnel concentrating solar collectors.” *Solar Energ.*, **103**, 639-652.
<https://doi.org/10.1016/j.solener.2013.05.021>.